

N89 - 15961

CORRELATIONS BETWEEN SOLAR ACTIVITY AND OPERATIONALLY DETERMINED  
SATELLITE DRAG VARIATION PARAMETERS\*

E. A. Smith, Computer Sciences Corporation (CSC)

ABSTRACT

Operational orbit determination of the Earth Radiation Budget Satellite (ERBS) and the Solar Maximum Mission (SMM) spacecraft using the Goddard Trajectory Determination System (GTDS) in the Flight Dynamics Facility (FDF) of the Goddard Space Flight Center (GSFC) has yielded an orbit solution data base of 3 years for ERBS and 8 years for SMM. One of the parameters in each data base is the drag variation parameter used in the GTDS atmospheric drag model; this parameter is solved for routinely to accommodate the different atmospheric densities as they are encountered solution to solution. These two data bases of the drag variation parameter solutions are analyzed to evaluate correlations in the variations of the parameter with changes in the 10.7-centimeter wavelength solar flux, F10.7, and the geomagnetic index.

The data for SMM span a wider range of solar flux values and show a stronger correlation. The data for ERBS, which is at a higher altitude and inclination than SMM, show a significant degree of scatter. For both satellites, the data indicate that changes in the drag variation parameter are more strongly correlated with the F10.7 solar flux than with the geomagnetic index. Correlations with the geomagnetic index are apparent only for severe geomagnetic storm conditions.

Results from this analysis enhance the understanding of the drag model and the accommodation of atmospheric density variations in operational orbit determination support. The resulting improvements in operations support procedures will be important for continued maintenance of the quality and accuracy of orbit solutions and propagations during periods of high solar flux. The results of this analysis for SMM have contributed directly to analysis currently being performed to predict the SMM reentry date.

---

\*This work was supported by the National Aeronautics and Space Administration (NASA)/Goddard Space Flight Center (GSFC), Greenbelt, Maryland, under Contract NAS 5-31500.

## 1. INTRODUCTION

Operational orbit determination at the Goddard Space Flight Center (GSFC) Flight Dynamics Facility (FDF) using the Goddard Trajectory Determination System (GTDS) has yielded a data base of orbit solutions for the Earth Radiation Budget Satellite (ERBS) that exceeds 3 years in length. Similarly, the data base of orbit solutions for the Solar Maximum Mission (SMM) spacecraft currently approaches 8 years in length. These solutions consist of six-parameter orbital state vectors, which represent the position and velocity vectors at the solution epoch, and an atmospheric drag force scaling parameter,  $\rho_1$ , called the drag variation parameter. This parameter is solved for routinely to accommodate differences between modeled and actual drag effects from solution to solution. The combined data bases of  $\rho_1$  solutions are analyzed in this paper to evaluate correlations in the variations of  $\rho_1$  with changes in the 10.7-centimeter wavelength solar flux (F10.7) and the geomagnetic index,  $A_p$ .

The degree of correlation of  $\rho_1$  with the solar flux values is evaluated in this paper to demonstrate the degree to which  $\rho_1$  actually accommodates changes in the atmospheric density relative to other phenomena, such as the geopotential model and tracking errors. Atmospheric density models correlate the atmospheric density with the F10.7 solar flux and the geomagnetic activity. The 10.7-centimeter (2800-megahertz) solar radio flux is reported from Ottawa, Canada, and is measured in units of  $10^{-22}$  watts per meter<sup>2</sup> per hertz. The geomagnetic index,  $A_p$ , is a measure of the amplitude of magnetic field disturbances based on a planetary average.

The F10.7 solar flux and  $A_p$  values reported over the period covered by this analysis were obtained from Solar-Geophysical Data Prompt Reports, published by the National Oceanic and Atmospheric Administration (NOAA) on a monthly basis. The values were entered into a master data base available for use for any spacecraft. The solar flux is characterized by smooth variations with a periodicity corresponding to the 27-day solar rotation.

The geomagnetic index is characterized by short intense bursts at random intervals, with the bursts sometimes being correlated with the solar rotation period.

The GTDS atmospheric drag force modeling, which includes the Harris-Priester atmospheric density model, is discussed in Section 2. Section 3 describes the orbit determination support procedures followed in the GSFC FDF for the ERBS and SMM spacecraft. The data analyses for ERBS and SMM are presented Sections 4 and 5, respectively. Section 6 gives the summary and conclusions for this study.

## 2. THE GTDS ATMOSPHERIC DRAG MODEL

In GTDS, the atmospheric drag force,  $\vec{F}_D$ , acting on a spacecraft is modeled by the following equation:

$$\vec{F}_D = -\frac{1}{2} \rho \vec{V}_r |\vec{V}_r| C_D A (1 + \rho_1) \quad (1)$$

where  $\rho$  = atmospheric density

$\vec{V}_r$  = velocity of the spacecraft with respect to the atmosphere

$C_D$  = spacecraft drag coefficient

$A$  = spacecraft reference cross-sectional area

$\rho_1$  = drag variation parameter, which is a scale factor error coefficient on the  $C_D \rho$  product

The density,  $\rho$ , is obtained in GTDS using the Harris-Priester atmospheric density model (References 2 through 4) in the form of 10 density profile tables (Tables HP1 through HP10) corresponding to 10 discrete values of the F10.7 solar flux. These tables provide minimum and maximum values of the atmospheric density at discrete altitude points. The Harris-Priester model averages the semiannual and seasonal-latitudinal variations, but it does

not attempt to account for the extreme ultraviolet 27-day effect or for variations in the geomagnetic index,  $A_p$ .

The GTDS atmospheric drag model also includes a diurnal bulge, which is a region of increased atmospheric density on the sunlit hemisphere of the Earth. The density variation due to the diurnal bulge is modeled as proportional to  $\cos^2(\alpha/2)$ , where  $\alpha$  is the angle between the spacecraft position vector and the apex of the diurnal bulge. The average density is the arithmetic average of the maximum value, which occurs at the apex of the diurnal bulge, and the minimum value, which occurs at the nadir of the diurnal bulge.

The profiles of the atmospheric densities for a range of altitudes relevant to the SMM mission are illustrated in Figure 1. Table 1 gives the Harris-Priester table numbers, the corresponding F10.7 solar flux values, and the range of solar flux values for which each table is used operationally.

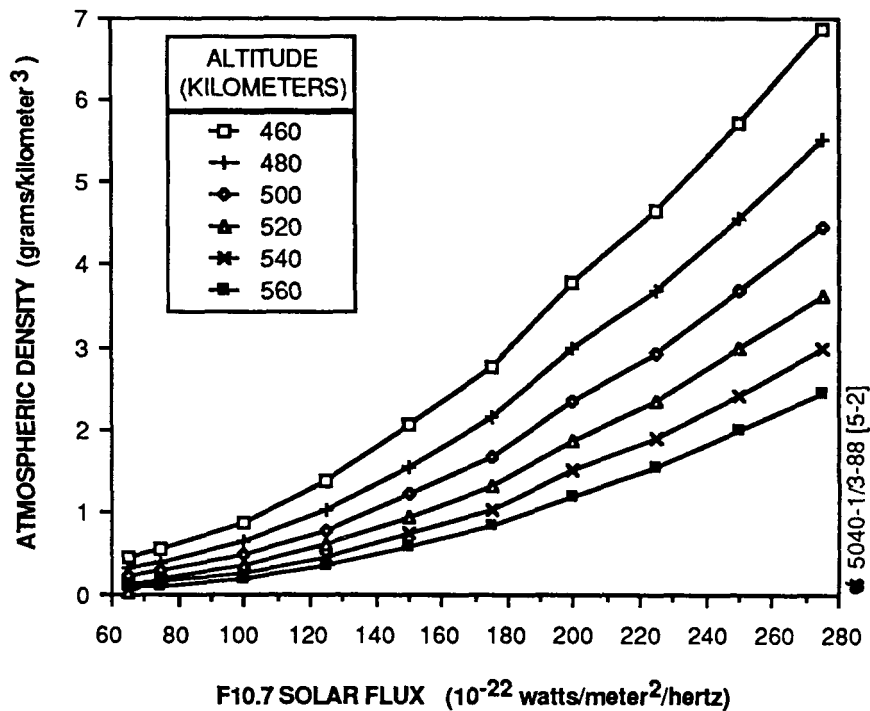


Figure 1. Harris-Priester Standard Atmospheric Densities as a Function of the F10.7 Solar Flux for Altitudes Relevant to SMM

Table 1. GTDS Harris-Priester Atmospheric Density Tables

HARRIS-PRIESTER (HP) TABLE NO.	F10.7 SOLAR FLUX VALUE ( $10^{-22}$ watts/meter <sup>2</sup> /hertz)	F10.7 SOLAR FLUX VALUE RANGE FOR HP TABLE OPERATIONAL USE ( $10^{-22}$ watts/meter <sup>2</sup> /hertz)
HP1	65	NOT USED
HP2	75	LESS THAN 88
HP3	100	88 - 112
HP4	125	113 - 137
HP5	150	138 - 162
HP6	175	163 - 187
HP7	200	188 - 212
HP8	225	213 - 237
HP9	250	238 - 262
HP10	275	263 - 287

5040-2/3-88 [5-2]

In the GTDS drag model, the drag variation parameter,  $\rho_1$ , is solved for in the differential correction process to accommodate drag variations relative to the nominal values provided by the Harris-Priester table and the spacecraft drag coefficient and to account for drag-like effects from other unmodeled perturbations. If drag is an important perturbing force on a spacecraft, it is necessary to solve for  $\rho_1$ , since the density tables corresponding to 10 discrete values of the solar flux cannot properly represent the density and resulting drag force for a continuum of solar flux values. The drag variation parameter,  $\rho_1$ , can therefore be utilized as a parameter for interpolating between the Harris-Priester tables to determine densities corresponding to intermediate values of the F10.7 solar flux.

For an F10.7 solar flux value less than 88, Harris-Priester Table HP2 (see Table 1 above), which is based on an F10.7 solar flux value of 75, is used operationally. For an F10.7 solar flux value between 88 and 112, Table HP3, based on an F10.7 solar flux value of 100, is used. Similarly, for

higher values of the solar flux, the closest standard table is used, as indicated in the last column of Table 1. Table HP1 is not used operationally.

### 3. ORBIT DETERMINATION SUPPORT PROCEDURES FOR ERBS AND SMM

Operational orbit support for ERBS consists of two orbit solutions per week, on Tuesday and Friday. The orbit solution on Tuesday uses a tracking data arc of 5 days and 10 hours, ending on Tuesday at 10 hours UTC. The Friday orbit solution uses a tracking data arc of 4 days and 10 hours, ending on Friday at 10 hours UTC. The geopotential model used is the Goddard Earth Model-9 (GEM-9), truncated to order and degree 8. The drag variation parameter,  $\rho_1$ , is solved for in each orbit solution, and the value obtained is used in the generation of two ephemerides: a 21-day ephemeris produced on each solution date and a 47-day ephemeris produced each Tuesday. In addition to these predicted ephemerides, a 1-week merged definitive ephemeris is prepared each week for delivery to the ERBS experimenters at NASA's Langley Research Center (LaRC).

Operational orbit support for SMM consists of an orbit solution every other day. These orbit solutions use a tracking data arc of 2 days and 10 hours. The geopotential model used is the GEM-9, truncated to order and degree 16, although over the history of SMM mission support values higher and lower than 16 have been used. The  $\rho_1$  parameter is solved for in each solution, and the value obtained is used in the generation of a 12-day ephemeris on each solution date and a 37-day ephemeris once a week. In addition, each 58-hour definitive ephemeris is delivered to the SMM experimenters.

To quality assure the solutions for each spacecraft, ephemeris comparison runs are made, using the GTDS Ephemeris Comparison (COMPARE) Program, on consecutive orbit solutions over the respective overlap intervals. The maximum position difference from this comparison is a measure of the consistency of the orbit solutions. A second quality check is made by

comparing the current orbit solution with an ephemeris propagated from the solution before last.

#### 4. ERBS DATA ANALYSIS

The ERBS orbit has maintained a nearly constant semimajor axis of 6981 kilometers (corresponding to an altitude of 603 kilometers) since the start of the mission in October 1984. During this period, the solar flux has been near the minimum of its 11-year cycle, and relatively low drag forces have been present. Although no significant orbital decay has occurred, the drag force is still considered to be an important perturbation, and  $\rho_1$  is solved for in the orbit solution. For spacecraft at higher altitudes (i.e., Landsat-4 and Landsat-5 at 700 kilometers and Nimbus-7 at 950 kilometers), the drag force becomes less significant and solving for  $\rho_1$  leads to nonphysical values.

The F10.7 solar flux and geomagnetic index values for the epoch dates of the ERBS orbit solutions are presented in Figure 2 for the period from October 1984 to October 1987. The corresponding  $\rho_1$  values from the operational orbit solutions are shown in Figure 3. Since more than one Harris-Priester table was used during this time period, the solved-for  $\rho_1$  data have been normalized to reflect the solved-for atmospheric density adjustment relative to Table HP2 (F10.7 solar flux value = 75) for an altitude of 600 kilometers.

To verify the normalization procedure, GTDS runs were made to determine the  $\rho_1$  differences that correspond to the difference between Tables HP3 and HP2. Using Table HP3 and a  $\rho_1$  value of -0.47 gave a zero along-track error at the end of the 1-day propagation when compared with an ephemeris using Table HP2 and a  $\rho_1$  value of 0.00. Similarly, using Table HP2 and a  $\rho_1$  value of +0.89 gave a zero along-track error after 1 day when compared with an ephemeris using Table HP3 and a  $\rho_1$  value of 0.00. These values are

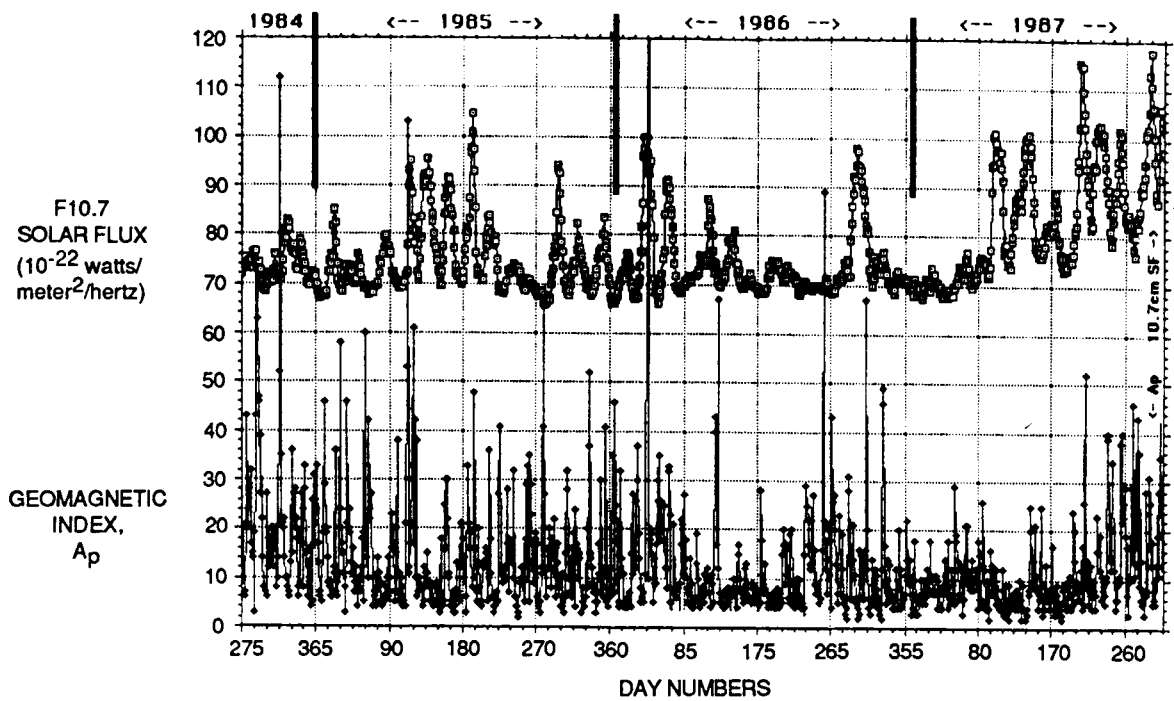


Figure 2. F10.7 Solar Flux and Geomagnetic Index Values for ERGS Orbit Solution Epoch Dates

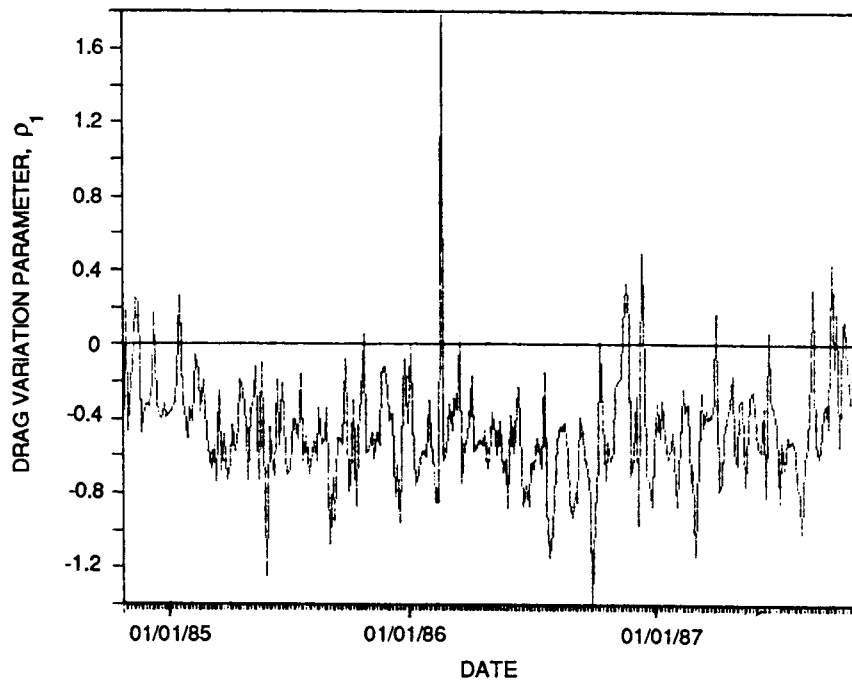


Figure 3. Drag Variation Parameter Values From ERBS Operational Orbit Solutions



consistent with those determined by taking the ratio of the average densities for an altitude of 600 kilometers from Tables HP2 and HP3.

Most of the operational  $\rho_1$  data were associated with Table HP2; the operational data associated with Table HP3 were converted to the equivalent for Table HP2 by the normalization procedure, which is described in Appendix A. Only the HP2 and HP3 tables were used for the ERBS study, since no F10.7 solar flux values above 112 were encountered during the 3 years covered by the ERBS data.

The normalized  $\rho_1$  values from the ERBS orbit solutions are plotted versus the F10.7 solar flux in Figure 4 and versus the geomagnetic index in Figure 5. No clear correlation can be seen from these plots. The correlation coefficients,  $R$ , are the following:  $R_{F10.7} = 0.182$  and  $R_{Ap} = 0.459$ . The data are characterized by a large amount of noise that obscures any evident trend. Possible reasons for the observed noise are the following:

1. Errors in the solved-for  $\rho_1$  due to the length of the tracking data arc
2. Errors in the F10.7 solar flux and geomagnetic index values used
3. Modeling errors with drag-like effects

To investigate the errors in  $\rho_1$  due to the tracking arc length, the  $\rho_1$  data were segmented into values from 4-day arcs and values from 5-day arcs. No significant difference was observed between the two samples. Specifically, the average value of  $\rho_1$  for the 4-day arcs was  $-0.4691$ , while for the 5-day arcs, the average value of  $\rho_1$  was  $-0.4613$ . Errors in the F10.7 solar flux or geomagnetic index values arise because the values used were the values on the solution epoch date and not on an average value over the tracking data arc. To evaluate these errors, the arithmetic mean of the F10.7 solar flux and geomagnetic index values over the tracking data

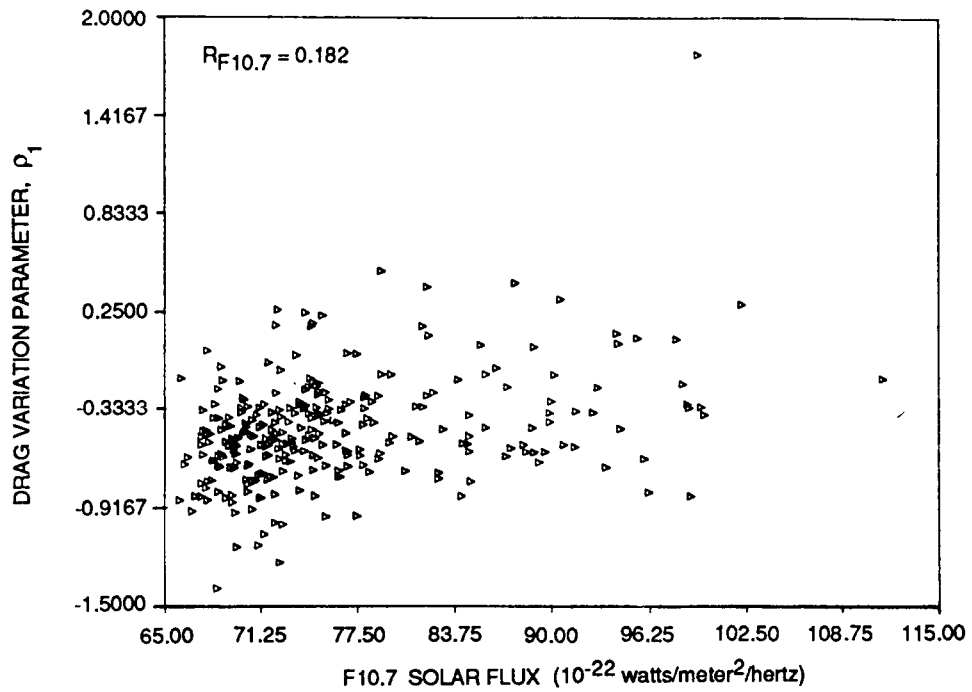


Figure 4. Normalized ERBS Drag Variation Parameter Values as a Function of the F10.7 Solar Flux From October 1984 to October 1987

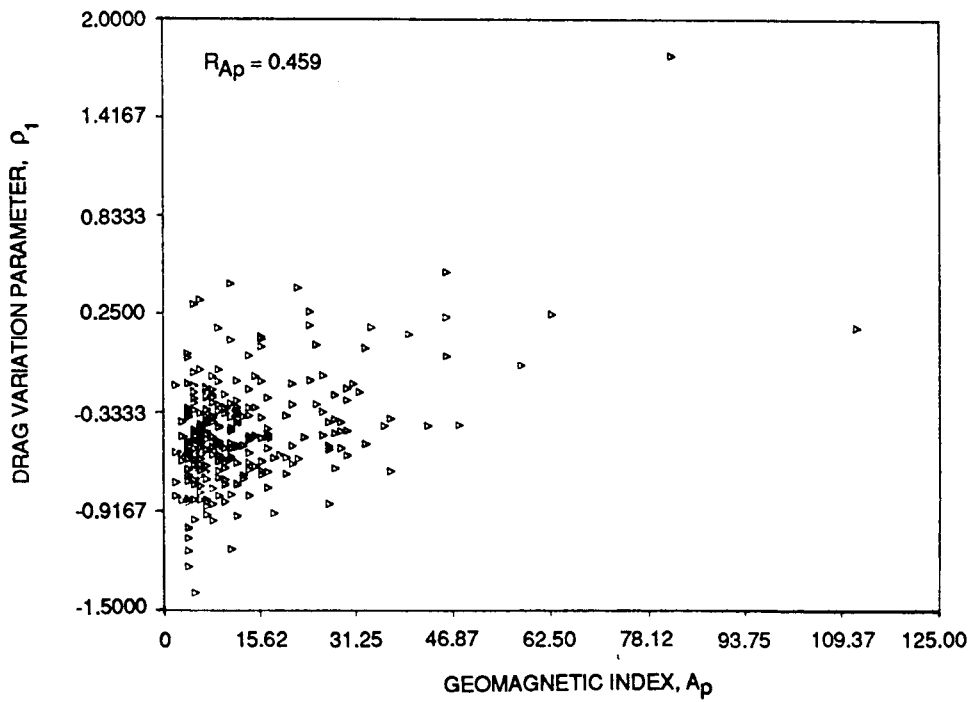


Figure 5. Normalized ERBS Drag Variation Parameter Values as a Function of the Geomagnetic Index From October 1984 to October 1987

arc were used rather than the values on the epoch date; only a slight reduction in the noise resulted. The F10.7 correlation coefficient,  $R_{F10.7}$ , increased slightly, from 0.182 to 0.235, when the arithmetic mean values were used. Likewise, the  $A_p$  correlation coefficient,  $R_{A_p}$ , increased from 0.459 to 0.559. It was therefore concluded that the noise appears to reflect modeling errors intrinsic to other factors in the propagation model and input data.

## 5. SMM DATA ANALYSES

The SMM orbit analysis is described in Section 5.1. Section 5.2 presents a description of a method to improve the drag model by adjusting the SMM drag coefficient. Section 5.3 discusses ephemeris propagation and reentry predictions for SMM.

### 5.1 SMM ORBIT ANALYSIS

SMM was launched on February 14, 1980, and by October 1987 the drag force had caused the semimajor axis to decay from 6952 kilometers (574 kilometers altitude) to 6865 kilometers (487 kilometers altitude). SMM orbit solutions from launch through the end of October 1987 have been used to study the effects of solar flux variations on the atmospheric density as estimated by the GTDS solved-for  $\rho_1$  values. For each orbit solution, the following are tabulated: (1) the observed values of the F10.7 solar flux and the geomagnetic index, (2) the Harris-Priester table used in the orbit solution, and (3) the solved-for value of  $\rho_1$ .

For consistency, all  $\rho_1$  values were normalized to reflect the empirical atmospheric densities, as was done for the ERBS data. Because the SMM altitude was rapidly decaying during the period several years ago when the solar flux was high, the conversion algorithm constants varied with the spacecraft altitude and, therefore, with the mission year. For specific

mission years, density table values corresponding to the spacecraft altitudes given below were used:

<u>Mission Year</u>	<u>Spacecraft Altitude (kilometers)</u>
1980	560
1981	540
1982	520
1983	500
1984	500
1985	480
1986	480
1987	480

Figure 1 shows the F10.7 solar flux as a function of the atmospheric density for each of these altitudes. The details of the conversion algorithm for SMM are given in Appendix B.

The empirical atmospheric densities for SMM are shown in Figure 6 as a function of the observed F10.7 solar flux on the epoch date. As expected, a clear correlation between the solar flux and the atmospheric density is evident in this figure ( $R_{F10.7} = 0.863$ ). The densities plotted as a function of the geomagnetic index,  $A_p$ , in Figure 7 show a weak correlation ( $R_{A_p} = 0.247$ ).

## 5.2 ADJUSTING THE SMM DRAG COEFFICIENT TO CALIBRATE THE DENSITY MODELING

A clear correlation between the atmospheric density and the observed F10.7 solar flux is demonstrated by the analysis presented in Section 5.1. For values of the F10.7 solar flux that lie between the Harris-Priester table values, an expected value of  $\rho_1$  can be determined by interpolation. The  $\rho_1$  values obtained from the operational orbit solutions average approximately -0.6, while those obtained by interpolating the Harris-Priester table values to the observed solar flux/average approximately 0.0; therefore,

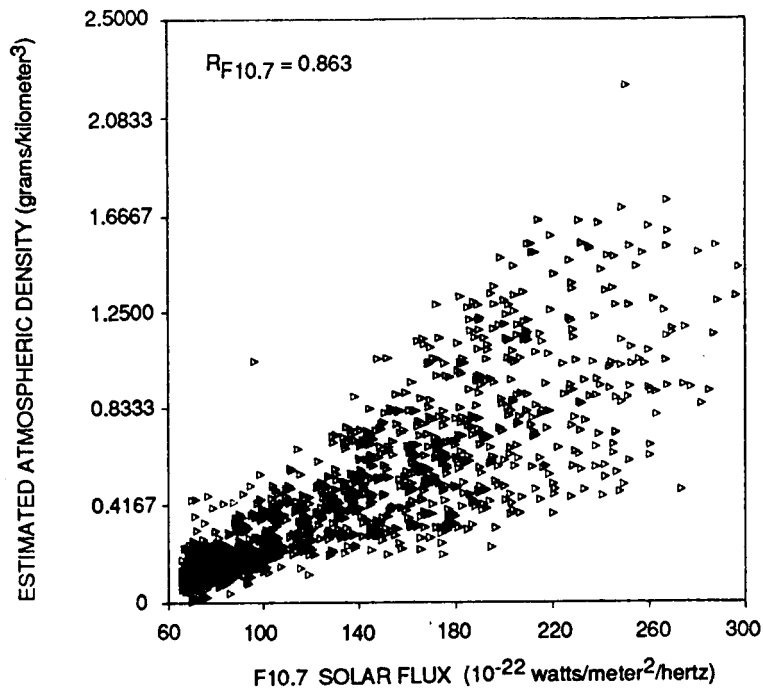


Figure 6. SMM Estimated Atmospheric Density as a Function of the F10.7 Solar Flux From Launch to October 1987

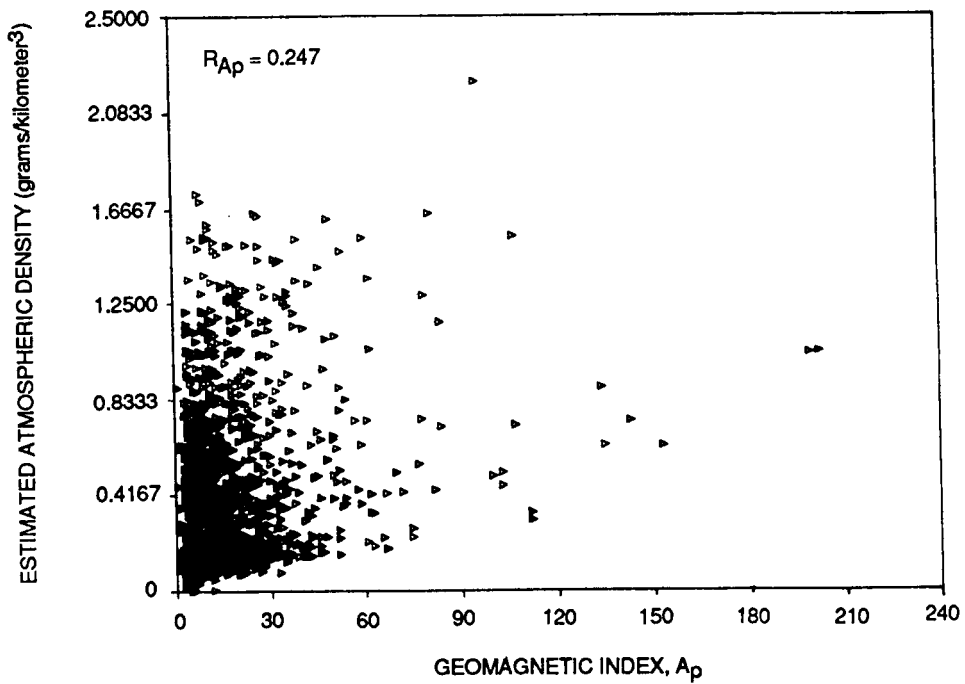


Figure 7. SMM Estimated Atmospheric Density as A Function of the Geomagnetic Index From Launch to October 1987

it is clear that the expected values are significantly different from those actually seen in the SMM orbit solutions. A likely source of this difference is the failure to account for attitude-dependent drag variations.

Since some of the error in the drag model originates from the time-dependence of the spacecraft attitude with respect to the relative velocity vector, the approach taken was to determine a value of the drag coefficient that results in  $\rho_1$  values near those expected from interpolating the Harris-Priester tables to the actual F10.7 solar flux level. This procedure effectively calibrates the drag modeling such that the term  $\rho (1 + \rho_1)$  provides a direct estimate of the actual atmospheric density.

Drag coefficient normalization was performed using the empirical densities derived from the solved-for  $\rho_1$  values. The drag coefficient value that results in atmospheric density values consistent with the solar flux levels in the range 150 to 200 was found to be 1.38. Further refinement of this result is possible using GTDS propagations and comparisons with past evolution of the SMM orbit during the previous solar maximum.

5.3 EPHEMERIS PROPAGATION AND REENTRY PREDICTIONS FOR SMM

Predictions of the monthly averages of the F10.7 solar flux are available from the Atmospheric Sciences Division, Marshall Space Flight Center (MSFC) (Reference 5). For the months April 1987 through January 1988, the actual observed monthly averages have been calculated and are in good agreement with the predicted averages (see Table 2). For each month in 1988 and 1989, the estimated monthly average F10.7 solar flux has been converted to an expected value of  $\rho_1$  for the appropriate Harris-Priester table, following the procedure described in Appendix B. Using the calibrated value of 1.38 for the drag coefficient, the SMM orbit was propagated using GTDS on a month-by-month basis. For each month, the selected Harris-Priester table and the expected  $\rho_1$  value (see Table 3) were incorporated into the drag model. The resulting ephemeris predicts that the SMM reentry will occur in February 1990.

Table 2. MSFC Predicted F10.7 Solar Flux and the Observed F10.7 Solar Flux From April 1987 Through January 1988

MONTH	F10.7 SOLAR FLUX VALUE ( $10^{-22}$ watts/meter <sup>2</sup> /hertz)	
	MSFC PREDICTED	OBSERVED
APRIL 1987	80.3	84.9
MAY 1987	82.3	87.8
JUNE 1987	84.5	77.9
JULY 1987	87.2	84.2
AUGUST 1987	90.7	90.0
SEPTEMBER 1987	94.2	86.1
OCTOBER 1987	97.8	98.1
NOVEMBER 1987	103.1	101.1
DECEMBER 1987	109.3	94.9
JANUARY 1988	115.3	108.8

5040-3/3-88 [5-2]

Table 3. MSFC Best-Estimate Monthly Average F10.7 Solar Flux, Selected Harris-Priester Table, and Expected Drag Density Variation Parameter From January 1988 Through February 1990

MONTH	MSFC BEST-ESTIMATE MONTHLY AVERAGE F10.7 SOLAR FLUX ( $10^{-22}$ watts/meter <sup>2</sup> /hertz)	HARRIS-PRIESTER TABLE NO.	$\rho_1$
JANUARY 1988	115.3	HP4	-0.1454
FEBRUARY 1988	121.7	HP4	-0.0495
MARCH 1988	128.4	HP4	0.0673
APRIL 1988	133.9	HP4	0.1761
MAY 1988	138.8	HP5	-0.1483
JUNE 1988	143.2	HP5	-0.0900
JULY 1988	148.3	HP5	-0.0225
AUGUST 1988	154.2	HP5	0.0652
SEPTEMBER 1988	160.4	HP5	0.1615
OCTOBER 1988	167.0	HP6	-0.0895
NOVEMBER 1988	172.9	HP6	-0.0235
DECEMBER 1988	178.2	HP6	0.0501
JANUARY 1989	182.7	HP6	0.1152
FEBRUARY 1989	187.9	HP7	-0.1317
MARCH 1989	191.6	HP7	-0.0915
APRIL 1989	194.1	HP7	-0.0642
MAY 1989	198.6	HP7	-0.0152
JUNE 1989	202.4	HP7	0.0215
JULY 1989	205.5	HP7	0.0493
AUGUST 1989	208.6	HP7	0.0771
SEPTEMBER 1989	210.0	HP7	0.0897
OCTOBER 1989	210.2	HP7	0.0915
NOVEMBER 1989	211.4	HP7	0.1022
DECEMBER 1989	212.9	HP8	-0.0886
JANUARY 1990	215.6	HP8	-0.0688
FEBRUARY 1990	218.1	HP8	-0.0505

5040-4/3-88 [5-2]



## 6. SUMMARY AND CONCLUSIONS

A study based on an operational data base of solved-for drag variation parameter values for 3 years of ERBS orbit solutions and 8 years of SMM orbit solutions has been presented in this paper. After adjustments to these data to account for variations in the associated Harris-Priester table, a clear correlation ( $R_{F10.7} = 0.863$ ) of the estimated atmospheric density with the F10.7 solar flux has been demonstrated for SMM. Thus, the inclusion of the solved-for  $\rho_1$  parameter in the orbital solution for SMM primarily accommodates the effects of drag on the orbit. In doing this, the solved-for  $\rho_1$  acts to interpolate the atmospheric density when the actual F10.7 solar flux values are between the values of the standard Harris-Priester tables; it also accommodates variations in the spacecraft effective drag coefficient resulting from daily science operations.

For ERBS, which is at a higher altitude and with solar activity levels near the solar minimum, no strong correlation was found between the estimated atmospheric density and the F10.7 solar flux or the geomagnetic index. The higher level of noise illustrated by the plots of  $\rho_1$  as a function of the F10.7 solar flux and the geomagnetic index indicate that for this spacecraft the solved-for  $\rho_1$  plays a large role in the accommodation of effects in the orbit propagation model that are not directly associated with atmospheric density and drag. One possible source of these errors is the effects of resonance of the spacecraft orbital period with geopotential harmonic coefficients.

As a part of the SMM study, the drag model was calibrated by adjusting the drag coefficient in such a way that densities estimated using the  $\rho_1$  values from the data base were in good agreement with density values obtained by interpolating the Harris-Priester table values. The results of this analysis have contributed directly to studies currently being performed in the orbit operations area of GSFC's FDF to predict the reentry date of the SMM. Estimates based on the calibrated SMM drag model and on the MSFC

predictions of the F10.7 solar flux levels indicate that SMM will reenter the atmosphere in February 1990. As indicated in Table 2, the most recent solar flux observations are lower than the MSFC predictions. If this trend continues, the SMM reentry will occur later than the February prediction.

APPENDIX A. DRAG VARIATION PARAMETER ( $\rho_1$ ) DATA  
STANDARDIZATION METHOD FOR ERBS

Assuming that the value of the spacecraft drag coefficient is correct and that there are no other modeling errors affecting the drag calculation, then the drag variation parameter,  $\rho_1$ , is a measure of the difference between the actual atmospheric density and the atmospheric density in the model being used. For example, a  $\rho_1$  value of -0.5 means 50 percent less atmospheric density, while a  $\rho_1$  value of +0.5 means 50 percent more atmospheric density, etc.

For the ERBS altitude (600 kilometers), the atmospheric density values for the HP2 and HP3 tables are given in Table 4. The table gives both a minimum and a maximum density.

Table 4. Harris-Priester Atmospheric Densities  
at an Altitude of 600 Kilometers

HARRIS-PRIESTER TABLE NO.	F10.7 SOLAR FLUX VALUE ( $10^{-22}$ watts/meter <sup>2</sup> /hertz)	ATMOSPHERIC DENSITY (kilograms/kilometer <sup>3</sup> )	
		MINIMUM	MAXIMUM
HP2	75	0.00001109	0.0001137
HP3	100	0.00002088	0.0002146

5040-5/3-88 [5-2]

Dividing the value from Table HP2 by the value from Table HP3 yields 0.53. The result is the same to two significant digits whether the minimum or maximum values are used.

Using the factor 0.53, the GTDS analysis results can be replicated. The atmospheric densities from Table HP2 are 47 percent less than those from Table HP3, so -0.47 is the theoretical  $\rho_1$  value for converting density values from Table HP3 to Table HP2. Similarly, the Table HP3 density values are 1.89 times as large as the Table HP2 values, or 89 percent more dense; thus, +0.89 is the theoretical  $\rho_1$  value for converting density values from Table HP2 to Table HP3.

The transformation equation can then be derived, making use of the fact that the actual atmospheric density is the same regardless of the Harris-Priester table being used. The density,  $\rho$ , is given by

$$\rho = (1 + \rho_1) \rho_0 \quad (\text{A-1})$$

where  $\rho_0$  is the tabulated density in the Harris-Priester table being used. The value from the Harris-Priester table is included as the argument of the variable. Equation (A-1) leads to the following expression:

$$\rho = [1 + \rho_1(2)] \rho_0(2) = [1 + \rho_1(3)] \rho_0(3) \quad (\text{A-2})$$

where the number in parentheses corresponds to the Harris-Priester table being used.

Next,  $\rho_1(2)$  can be solved for as

$$\rho_1(2) = \frac{\rho_0(3)}{\rho_0(2)} [1 + \rho_1(3)] - 1 \quad (\text{A-3})$$

Using the actual density ratio for ERBS yields

$$\rho_1(2) = 1.89 [1 + \rho_1(3)] - 1 \quad (\text{A-4})$$

APPENDIX B. DRAG VARIATION PARAMETER ( $\rho_1$ ) DATA  
STANDARDIZATION METHOD FOR SMM

The standardization procedure used for ERBS (Appendix A) was inadequate for standardizing the SMM data for the following reasons:

1. The SMM data require the use of Harris-Priester tables ranging from Table HP2 to HP10. With such a large spread, standardization to a single table would result in a loss of precision.
2. More than one altitude was encountered in the SMM data, and the conversion factor ratios are altitude dependent.
3. At the lower altitudes, different ratios are obtained depending on whether the minimum or maximum tabulated densities are used. This requires the determination of an average density.

The average value for the atmospheric density was determined to be the arithmetic mean of the maximum and minimum densities. This is established by integrating the cosine-squared dependence over a diurnal cycle, as follows:

$$\frac{1}{\pi} \int_0^{\pi} \cos^2 \theta \, d\theta = \frac{1}{2\pi} \int_0^{\pi} (1 + \cos 2\theta) \, d\theta = \frac{1}{2\pi} \left[ \theta + \frac{1}{2} \sin 2\theta \right] \Big|_0^{\pi} = \frac{1}{2} \quad (\text{B-1})$$

The empirical density is then calculated by taking the average density for the Harris-Priester table being used and multiplying it by the factor  $(1 + \rho_1)$ .

A further refinement in the analysis is to use the average densities to calculate expected  $\rho_1$  values for values of the F10.7 solar flux between the table values. The average densities and interpolating values of  $\rho_1$  are given in Table 5. The  $\rho_1$  (UP) column gives the value of  $\rho_1$  that accounts for a step up to the next highest Harris-Priester table. It is determined by

$$\frac{\rho(\text{HP}+1)}{\rho(\text{HP})} - 1$$

The  $\rho_1$  (DOWN) column contains the value of  $\rho_1$  that accounts for a step down to the next lowest Harris-Priester table. It is determined by

$$\frac{\rho(\text{HP}-1)}{\rho(\text{HP})} - 1$$

To determine a value of  $\rho_1$  given a value of the F10.7 solar flux, the difference between the given F10.7 solar flux value and the standard value for the table ( $\Delta\text{F10.7}$ ) is divided by 25 (the spacing between tables) and is then multiplied by the appropriate interpolating value of  $\rho_1$ . For example, for the case where the F10.7 solar flux is 115.3 and SMM is at 480 kilometers altitude, the following determination is made:

1. The given F10.7 solar flux value of 115.3 is closest to the solar flux value of 125 for Harris-Priester Table HP4, but is lower than the table value.
2. The expected  $\rho_1$  is then determined as

$$\rho_1 = \frac{125 - 115.3}{25} (-0.3745) = -0.1454 \quad (\text{B-2})$$

Table 5. Average Atmospheric Densities and Drag Variation Parameter Values to be Used for Interpolation

ALTITUDE (kilometers)	HARRIS- PRIESTER TABLE NO.	F10.7 SOLAR FLUX VALUE ( $10^{-22}$ watts/ meter <sup>2</sup> /hertz)	AVERAGE ATMOSPHERIC DENSITY (grams/kilometer <sup>3</sup> )	INTERPOLATING VALUES OF $P_1$	
				$P_1$ (DOWN)	$P_1$ (DOWN)
560	HP2	75	0.1112	-0.2054	0.8210
	HP3	100	0.2025	-0.4509	0.7353
	HP4	125	0.3514	-0.4237	0.6417
	HP5	150	0.5769	-0.3909	0.4287
	HP6	175	0.8242	-0.3000	0.4596
	HP7	200	1.203	-0.3149	0.2793
	HP8	225	1.539	-0.2183	0.2833
	HP9	250	1.975	-0.2208	0.2415
	HP10	275	2.452	-0.1945	0.1945
	540	HP2	75	0.1501	-0.2001
HP3		100	0.2680	-0.4399	0.7015
HP4		125	0.4560	-0.4123	0.6132
HP5		150	0.7356	-0.3801	0.4111
HP6		175	1.038	-0.2913	0.4422
HP7		200	1.497	-0.3066	0.2685
HP8		225	1.899	-0.2117	0.2728
HP9		250	2.417	-0.2143	0.2333
HP10		275	2.981	-0.1892	0.1892
520		HP2	75	0.2042	-0.1983
	HP3	100	0.3568	-0.4277	0.6676
	HP4	125	0.5950	-0.4003	0.5857
	HP5	150	0.9435	-0.3694	0.3916
	HP6	175	1.313	-0.2814	0.4265
	HP7	200	1.873	-0.2990	0.2568
	HP8	225	2.354	-0.2043	0.2630
	HP9	250	2.973	-0.2082	0.2254
	HP10	275	3.643	-0.1839	0.1839
	500	HP2	75	0.2798	-0.1873
HP3		100	0.4782	-0.4149	0.6338
HP4		125	0.7813	-0.3879	0.5577
HP5		150	1.217	-0.3580	0.3739
HP6		175	1.672	-0.2721	0.4085
HP7		200	2.355	-0.2900	0.2467
HP8		225	2.936	-0.1979	0.2524
HP9		250	3.677	-0.2015	0.2170
HP10		275	4.475	-0.1783	0.1783
480		HP2	75	0.3863	-0.1802
	HP3	100	0.6455	-0.4015	0.5988
	HP4	125	1.0320	-0.3745	0.4952
	HP5	150	1.543	-0.3312	0.3882
	HP6	175	2.142	-0.2796	0.3917
	HP7	200	2.981	-0.2814	0.2352
	HP8	225	3.682	-0.1904	0.2423
	HP9	250	4.574	-0.1950	0.2081
	HP10	275	5.526	-0.1723	0.1723

5040-6/3-88 [5-2]

## REFERENCES

1. Goddard Space Flight Center, X-582-76-77, Mathematical Theory of the Goddard Trajectory Determination System, A. J. Fuchs, C. E. Velez, and J. O. Cappellari, Jr. (editors), April 1976
2. Harris, I. and W. Priester, "Time Dependent Structure of the Upper Atmosphere," Journal of Atmospheric Sciences, Vol. 19, No. 4, July 1952
3. Goddard Space Flight Center, NASA-TN-D-144, Theoretical Models for the Solar Cycle Variation of the Upper Atmosphere, I. Harris and W. Priester, August 1962
4. Harris, I. and W. Priester, "Atmospheric Structure and Its Variations in the Region From 120 to 80 KM," COSPAR International Reference Atmosphere (CIRA) 1965, Space Research IV. Amsterdam, Holland: North Holland Publishing Company, 1965
5. Marshall Space Flight Center, Memorandum EL01 (184-87), Solar Activity Inputs for Upper Atmospheric Models Used in Programs to Estimate Spacecraft Orbital Lifetime, G. D. Hopson, October 14, 1987